Seismic Vulnerability Analysis of Wharf Structures using Artificial Neural Networks

A. Calabrese
ROSE School – IUSS Istituto Universitario di Studi Superiori, Pavia, Italy
C.G. Lai
University of Pavia, and EUCENTRE, European Centre for Training and Research in Earthquake Engineering, Italy

SUMMARY:
The research illustrates the use of Artificial Neural Networks (ANN) in the general framework of a performance-based seismic vulnerability evaluation for earth retaining structures. A fully nonlinear finite difference software is used to perform extensive time histories analyses of a prototype configuration for different earthquake intensity levels. Model input parameters are sampled according to their statistical distribution, and the seismic input is also considered as a random variable. With this process, a large dataset of virtual realizations of the behaviour of different configurations under recorded ground motions is obtained. The dataset is used to create ANNs capable of finding the unknown nonlinear relationship between seismic and geotechnical input data versus the expected performance of the facility. Once the ANN is calibrated, it can be effectively used as a "closed-form solution" to predict the seismic demand on the structure. Finally, fragility curves are systematically derived by applying Monte Carlo simulation on the obtained relationship.

Keywords: Artificial Neural Networks (ANN), Monte Carlo Simulation (MCS), Fragility Curves, Gravity walls

1. INTRODUCTION

A port infrastructure is a system that features: i) wharves (for berthing); ii) cranes (for loading/unloading operations); and iii) apron and internal ways (for allowing wheeled vehicles to reach the waterfront zone). This study is focused on assessing the seismic vulnerability of a specific quay wall typology, the blockwork construction, which is the oldest configuration of wharf structures around the world. The proposed methodology is also applied to an important Italian facility, the Port of Gioia Tauro, located in an active seismic region.

1.1. Case Study Description

The blockwork quaywall configuration used in this work as prototype structure consists of a set of five blocks, each with a height of 2.5 m, for a total height of 12.5 m, and a width from 8 m to 4 m, decreasing of 1 m for each level (Figure 1). This represents a typical realization technique widely used in Mediterranean Countries.

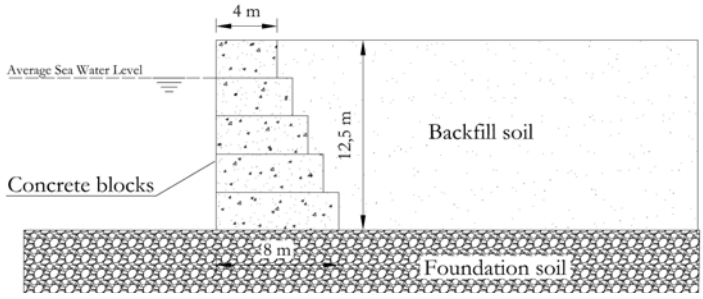

Figure 1. General model of the blockwork wharf analyzed in this study

The geotechnical characterization at the site (Scarpelli and Piersigilli, 2005) revealed that the soils are essentially cohesionless, with typical properties reported in Table 1.1.

Table 1.1. Soil properties assumed for the different stratigraphies based on (Scarpelli and Piersigilli, 2005)

Lithological unit	Depth [m]	γ [kN/m^3]	c' [N/m^2]	ϕ' [°]	E' [kN/m^2]
Sand with gravel	0-5	17	0	30	30000
Silty sand	5-12.5	19	0	30	50000
Coarse sand	12.5	18	0	36	50000
Fine sand	>12.5	19	0	36	80000

Uniform Hazard Spectrum (UHS) and deaggregation at the site were obtained from previous work done by the Italian Institute of Geophysics and Volcanology (INGV). The UHS for different probabilities of exceedance in 50 years are illustrated in Figure 2. For each return period, a set of seven spectrum compatible accelerograms has then been selected with the software ASCONA (Corigliano *et al.*, 2012).

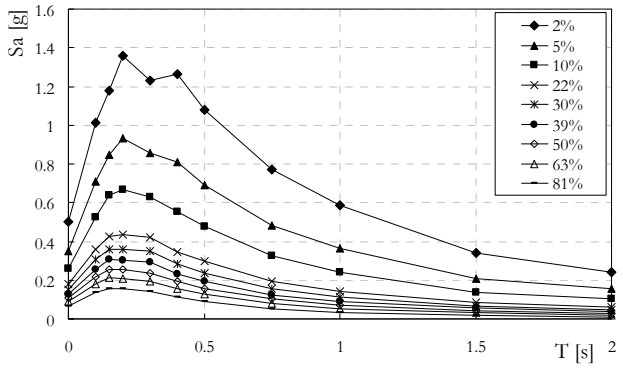

Figure 2. Uniform Hazard Response Spectra of pseudo-accelerations at the site for different probabilities of exceedance (from 2% to 81%) in 50 years

1.2. Numerical Modelling

The seismic response of the blockwork wharf was investigated by means of an advanced software, capable of modelling the nonlinear behaviour of geotechnical systems. FLAC 2D (Itasca, 2000) is a two-dimensional explicit finite difference program suitable for geotechnical engineering applications. It allows simulating the behaviour of structures interacting with soils, rock or other geomaterials that may undergo plastic deformation when exceeding their yield stresses. A large portion of the domain surrounding the wharf has been included in the model, in order to reproduce free-field conditions far away from the wall (Figure 3). These are further guaranteed by the presence of purposely-designed absorbing boundaries. The total mesh dimensions are 90 m by 42.5 m. In the vertical dimension, this allows to model the entire backfill and 30 m of the foundation soil. In the horizontal direction, the soil in front of the toe of the wall is modelled for a length of 26 m, while the backfill is modelled for a length of 56 m. A suitable grid is also selected to propagate the frequencies of interest.

After defining the geometry of the model, the materials have been assigned with a staged construction of the wall and with the geostatic stress initialization of the soil deposit. A hysteretic, Mohr-Coulomb constitutive model is used. The Seed *et al.* (1986) modulus reduction curve for sand has been used in order to take into account the soil nonlinear behaviour before yielding. A low amount of Rayleigh viscous damping, 0.2 %, centred at a frequency of 5 Hz (close to the fundamental frequency of the system) has also been added to eliminate high frequency noise and to simulate energy losses of the soil undergoing low-strain cyclic excitations. Lysmer and Kuhlemeyer (1969) viscous boundary to reproduce an absorbing (quiet) boundary were used at the bottom of the model, while free field conditions were assumed along the vertical boundaries. The hydrodynamic effects exerted by the

water pool on the seaward face of the wharf are addressed in the model using Westergaard's added masses (Westergaard, 1933). The dynamic pore pressure increment, together with shear strength decrease under seismic excitation, has been simulated with the Finn model (Martin *et al.*, 1975) using the Byrne formulation (1991). For further information on the adopted numerical simulation, the interested reader can refer to (Calabrese and Lai, 2012).

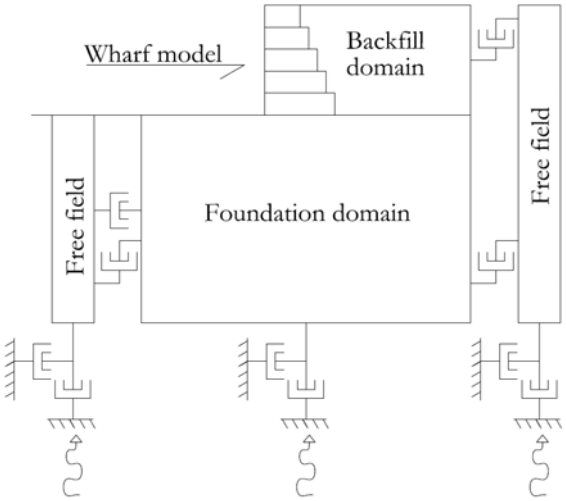

Figure 3. Model for seismic analysis of blockwork wharf structure with assigned boundary conditions

1.3 Performance Parameters

The damage criteria given by the International Navigation Association (PIANC, 2001) were used in order to assess the performance of the analyzed prototype configurations. Two damage mechanisms were considered: horizontal sliding and overturning failures. Therefore, the Engineering Demand Parameters (EDP) monitored after the numerical analyses were the normalized residual displacement on top of the quay wall (d/H) and the residual tilting towards the sea. PIANC (2001) also recommends acceptable levels of damage (Table 1.2), for different class of structures (according to their importance: from critical/strategic ports to small, easily restorable, facilities).

Table 1.2. Acceptable level of damage in performance-based evaluations adapted from PIANC (2001)

Level of damage	Structural	Operational
Degree I: Serviceable	Minor or no damage	Little or no loss of serviceability
Degree II: Repairable	Controlled damage	Short term loss of serviceability
Degree III: Near collapse	Extensive damage in near collapse	Long-term or complete loss of serviceability
Degree IV: Collapse	Complete loss of structure	Complete loss of serviceability

For blockwork wharves, the minimum EDP requirements for the damage levels listed in the table above are summarized in Table 1.3.

Table 1.3. Minimum requirements for damage criteria for gravity quay walls from PIANC (2001)

	Degree I	Degree II	Degree III	Degree IV
Normalized RHD	<1.5%	1.5~5%	5~10%	>10%
Residual tilting	<3°	3~5°	5~8°	>8°

2. USE OF AN ARTIFICIAL NEURAL NETWORK AS DEMAND EVALUATOR

2.1. Introduction to Artificial Neural Networks

An Artificial Neural Network (ANN) can be described as a massively parallel, interconnected network of basic computing elements that demonstrate information-processing characteristics similar to several hypothesized models of the functioning of the brain. Analogously to biological nervous systems, ANNs are in fact composed by simple elements operating in parallel. These elements are the "nodes" of the network, and each of them is associated with a specific "weight" and a specific "bias". The nodes are divided into several levels: input, hidden and output layers. The connections between the nodes are provided by particular "transfer functions" (also called "activation functions"), defining the decision that takes place within each node. Figure 4 represents the similarity between a schematized representation of a biological nervous system versus a topological depiction of an ANN.

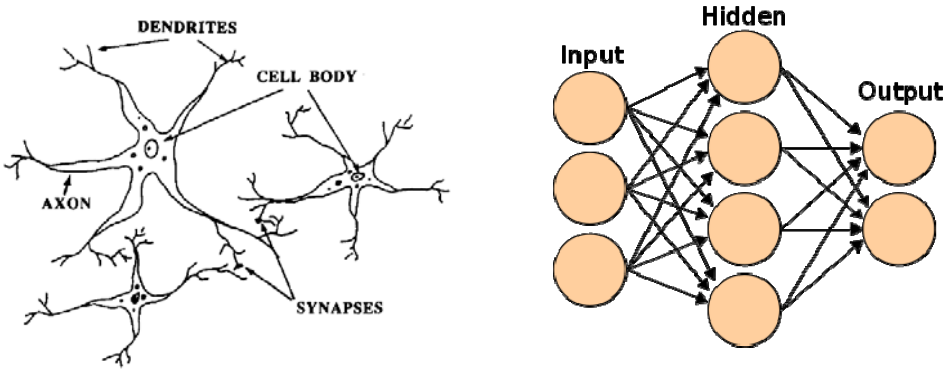

Figure 4. On the left, a schematized representation of a biological neuron based on (Hajela and Berke, 1992); on the right a topological depiction of an ANN

Artificial Neural Networks have nowadays several applications, as for instance in regression analyses, data clustering, data compression techniques, mapping rules. When solving complicated problems, an ANN can be particularly useful to find the unknown nonlinear relationship between a set of input data and a set of output values. In fact, while in a traditional multivariate regression analysis the type of the fitting function is assumed, with an ANN the type of interpolating function is not *a priori* assumed, being an outcome of the training process of the network.

For the above reason, an ANN is used in this study for performing the regression analysis linking the seismic, geotechnical and structural information of the wharf model to its expected seismic performance. This is evaluated according to the EDP thresholds already described in Section 1.3 (Table 1.2 and Table 1.3).

2.2. Obtaining the Dataset to Calibrate the ANN

The numerical FLAC model illustrated in Section 1.2 was used to perform a large number of parametric analyses. In these, all the input parameters are changed, and several natural ground motion records are utilized to perform dynamic time history analyses. The following six geotechnical parameters are deemed to be influential on the response of the model: i) the friction angle of the backfill soil; ii) the friction angle of the foundation soil; iii) the friction angle of the interfaces between the blocks and the backfill soil; iv) the friction angle of the interface between the base of the block with the underlying foundation soil; v) the small-strain shear modulus of the foundation soil; vi) and the small-strain shear modulus of the backfill soil. The seismic intensity was taken into account noting the Peak Ground Acceleration (PGA), Peak Ground Velocity (PGV), and Arias Intensity (IA) of the records used for the numerical simulations. The choice of such Intensity Measures (IMs) was adopted recalling the well know limitations of the PGA as an effective predictor of the seismic demand.

Nine sets of seven spectrum-compatible records were used, one for each of the probabilities of exceedance in 50 years indicated in Figure 2. The probabilities correspond to return periods ranging from 30 to 2457 years. Within each return period, uniform distribution is associated with the records. The uncertainty in the geotechnical properties was addressed by considering literature distributions of their values, as reported in (Jones *et al.*, 2002). Friction angles were therefore modelled with a normal distribution and a Coefficient of Variation (CoV) of 9%. The shear moduli, on the other hand, were modelled with a lognormal distribution and a CoV of 12%.

A MATLAB (The MathWorks, 2007) script was then created to generate the random geotechnical stratigraphies in FLAC and to make the correspondence with a randomly selected ground motion.

Nonlinear dynamic analyses were performed on such models and the output stored to be successively accessed. The entire process was repeated for different foundation's length, more precisely for 8 m, 11 m and 14 m, corresponding to base-length/height ratios around 0.64, 0.88 and 1.12. Thirty input files were generated for each intensity level, and the process was repeated for each geometrical configuration. Consequently, 810 time history analyses were performed. This required a large amount of computational time, approximately 1000 hours.

2.3. Architecture of the ANN

A feed-forward ANN model was used, together with the back-propagation algorithm for the training.

The term backpropagation is an abbreviation for "backwards propagation of errors", that is effective in summarizing the process that is implemented. In fact, the basic idea is that each hidden and output neuron processes its inputs by multiplying each input by its weight, summing the product and then passing the sum through a nonlinear transfer function to produce a result. The neural network learns by modifying the weights of the neurons in response to the errors between the actual output values and the target output values. This is carried out through a gradient descent on the sum of squares of the errors for all the training patterns. The process requires several iterations, whose number can vary depending on the adopted gradient descent algorithm. The single iteration is called a "cycle" or "epoch". Training is carried out by repeatedly presenting the entire set of training patterns (with the weights updated at the end of each cycle) until the error over all the training patterns is minimized and within the tolerance specified for the problem. Such type of network is defined as "feed-forward", as there is no feedback, i.e. no corrections, on the single loop.

An ANN model with 10 input nodes, a single hidden layer of 30 nodes, and 2 output nodes was adopted. The input nodes were the 6 geotechnical quantities and the 3 IMs listed in Section 2.2, as well as the geometrical aspect ratio of the wharf (W/H). The number of nodes in the hidden layer was found after a trial-and-error process, since it provided stable solutions without affecting the training time. The two output nodes give the RHD and the tilt of the quay wall.

The hidden layer was characterized with a tan-sigmoid transfer function (Figure 5, a), and the output layer with a linear one (Figure 5, b).

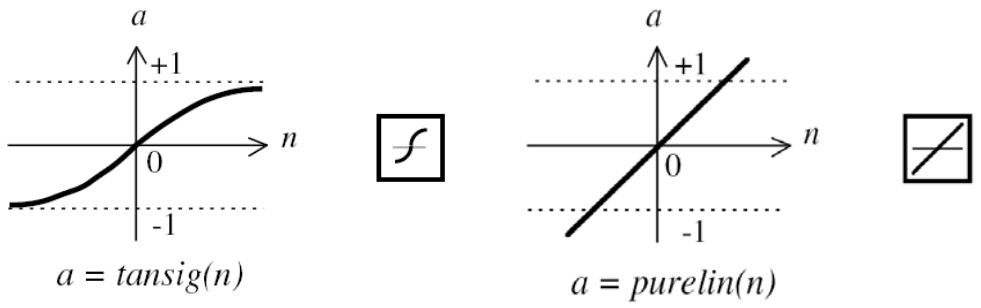

Figure 5. Tan-sigmoid transfer function (a); linear transfer function (b) (Demuth and Beale, 2004)

The topology of the ANN is represented in Figure 6 . In the illustration, LW is the weight matrix of the input vector, IW is the weight matrix of the output vector, K is the input matrix, b^1 and b^2 are the bias matrices.

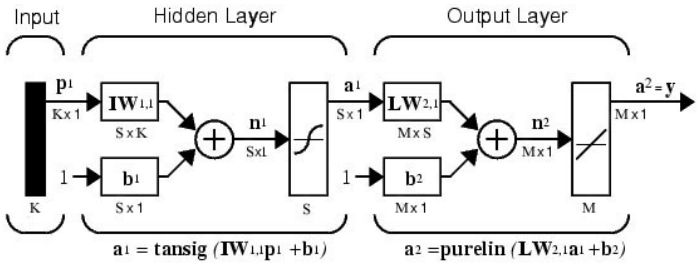

Figure 6. Architecture of the ANN used in this study (Demuth and Beale, 2004)

2.4. Training the ANN

The Levenberg-Marquardt algorithm was used for training. In addition, in order to improve generalization and to avoid overfitting, an early-stopping technique was also adopted. With this approach, the available data is divided into three subsets. The first subset is the training set, which is used for computing the gradient and updating the network weights and biases. The second subset is the validation set. The error on the validation set is monitored during the training process. The validation error will normally decrease during the initial phase of training, as does the training set error. However, when the network begins to overfit the data, the error in the validation set will typically begin to rise. When the validation error increases for a specific number of iterations, the training is stopped, and the weights and biases at the minimum of the validation error are returned.

Therefore, of the 810 known input-output realizations obtained with the numerical simulations, the 50% of the set was used to calibrate the ANN, the 25% to validate it, and the remaining 25% for testing. Figure 7 graphically illustrates the correlation obtained on the testing set after the training of the network.

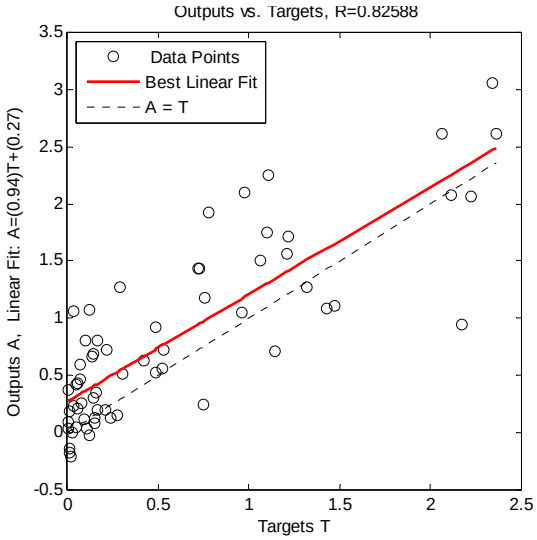

Figure 7. Graphical representation of the correlation obtained on the testing set after the training process

The matrices involved in the solution algorithm are stored. In this way, the seismic response of a wharf configuration with any input parameters (provided that these fall in the range used for determining the training set) can be determined with an algebraic “closed-form” solution of the type:

$$T = LW \cdot \tan sig(IW \cdot K + B_1) + B_2 \tag{2.1}$$

where LW is the weight matrix of the input matrix used to calibrate the ANN (hidden x input), IW is the weight matrix of the output vector used to calibrate the ANN (hidden x output), K is the input matrix (used to generate the solution), B_1 is the bias matrix of the hidden layer level, and B_2 is the bias of the output layer level.

Knowing all the above matrices, the relationship in Equation (2.1) can be regarded as a "metamodel". In other words, it can be used as a simple tool to estimate the output of a complicated problem.

3. DERIVATION OF FRAGILITY CURVES WITH ANN

Fragility curves represent the conditional probability, for a particular construction, of exceeding a defined level of damage. The probability is conditional on a given level of ground motion. Several references illustrate the fundamentals of fragility curves, amongst them Rota (2007) and Shinozuka *et al.* (2000). Even if the discussion of the proposed methodology is limited to these particular structures, it can be easily applicable to any other construction typology. The basic idea is to use the closed form solution obtained with the application of the ANN to generate a large number of simulations and to assess for each of them the reached damage state (DS). This knowledge is successively used to generate the fragility curves with a suitable regression analysis.

The main advantage of such method is a significant reduction in computational time, because no more nonlinear time history analyses are required once the network is calibrated. In the specific case, the FLAC model is used only at an initial stage to obtain data to train and validate the ANN. The classical alternative way would be to perform MCS directly on the input of the FLAC model, and then running the analyses. Since MCS requires at least thousands of analyses, and each time history analysis in FLAC lasts some hours, it is evident that this approach would be extremely computationally expensive. In fact, thousands of computing hours would be needed to perform the MCS. Conversely, the ANN approach is incomparably faster, since the deterministic model that is applied every time is just an algebraic expression. In this way, MCS can be run only in few minutes.

3.1. Uncertainties Considered in the Fragility Curves

3.1.1. Geotechnical Parameters

Each model geotechnical parameter (i.e. soil friction angles, low-strain shear moduli, friction angles at the interfaces) was modelled as a random variable with its specific distribution (see also Section 2.2). Once the random variables distributions were defined for what concerns the geotechnical parameters, an appropriate sampling was adopted in order to consider the different configurations of the wharf model.

3.1.2. Ground Motion Characteristics

Fragility curves can be developed for several intensity measures. Generally speaking, in structural earthquake engineering the most common choices are the PGA and the spectral acceleration at the fundamental period of the structure, $Sa(T_1)$. Also in geotechnical earthquake engineering the PGA is one of the preferred IMs for the construction of fragility curves, together with the PGV, PGD and AI. The ANN developed in this study characterizes the ground motion with three significant parameters: PGA, PGV, and IA. Hence, the probability of failure expressed by the fragility curve was conditioned on the PGA. At the same time, the other two parameters, PGV and IA, are also treated as random variables in order to consider the record-to-record variability. This was performed by defining the joint probability distribution (pdf) of PGA and PGV, as well as of PGA and IA. Recent studies, e.g. (Baker, 2007), have shown that the hypothesis of joint lognormal distribution between PGA and PGV and PGA and IA cannot be rejected. Therefore, a joint normal distribution was established between the logarithms of PGA and PGV and between the logarithms of PGA and IA. In the following discussion

the analytical formulas will only be given for the PGA and PGV distribution, however identical steps and logic also apply for PGA and IA.

Having defined a lognormal distribution between the probabilities of PGA and PGV, random variables indicated herein as A and V for conciseness, the logarithmic mean λ_A and logarithmic standard deviation ζ_A are assigned for A, as well as λ_V and ζ_V for V:

$$f_{A,V}(a,v) = \frac{1}{2\pi\zeta_A\zeta_V\sqrt{1-\rho^2}} \cdot \exp\left[\frac{-1}{2(1-\rho^2)} \cdot \left\{\left(\frac{\ln a - \lambda_A}{\zeta_A}\right)^2 - 2\rho\left(\frac{\ln a - \lambda_A}{\zeta_A}\right)\left(\frac{\ln v - \lambda_V}{\zeta_V}\right) + \left(\frac{\ln v - \lambda_V}{\zeta_V}\right)^2\right\}\right] \tag{3.1}$$

where ρ is the correlation coefficient between A and V.

The joint pdf between PGA and PGV used in this work (Figure 8) was therefore obtained based on their marginal distributions, using a correlation coefficient of 0.65 from existing literature, e.g. (Rathje and Saygili, 2008). For what concerns the marginal distributions, these were found from the hazard curves as, for instance, in Lee and Mosalam (2005).

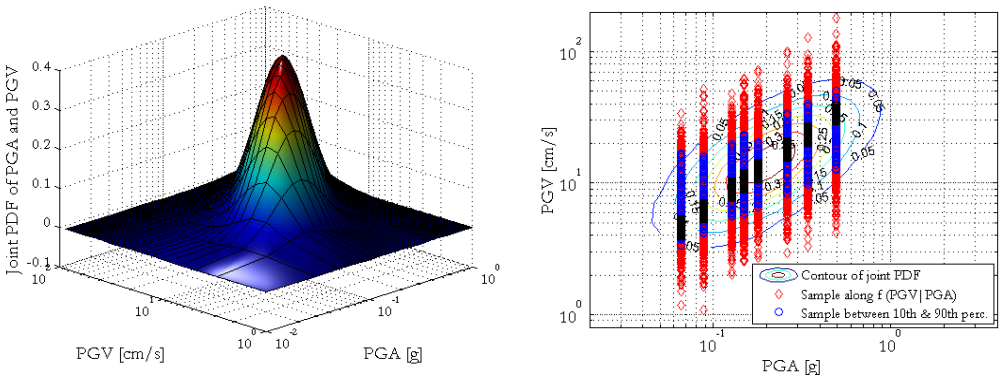

Figure 8. Joint lognormal distribution of PGA and PGV used in this study (a); and contour lines of the joint pdf, with superimposed random realizations of PGV conditional to a given PGA level.

A similar approach was also used in determining the joint pdf of PGA and IA. A complete description of the procedure can be found in (Calabrese and Lai, 2012).

3.2. Generation of Fragility Curves

Having defined the statistical distributions of all the input variables, the ANN closed-form solution was used in conjunction with MCS, to obtain a very large set of expected responses. For each PGA level a sample of 1000 random realizations (input-output) was obtained, and the computed RHD and tilt were stored and compared with the damage thresholds defined by PIANC (2001).

For each Damage State (DS) the number of failures is recorded during the MCS, so that the observational frequency $\hat{P}$ is easily obtained as the number of failure events N_f over the total number of simulations N, Equation (3.2):

$$P_f \approx \hat{P}_f(N) = \frac{1}{N} \cdot \sum_{i=1}^{N} I_f(x_i) = \frac{N_f}{N} \tag{3.2}$$

where $I_f(x_i)$ is a counter of the number of realizations, and its value can be either 1 or 0.

In this study, the classical assumption that the shape of the fragility function is well described by a lognormal CDF, e.g. (Shinozuka *et al.*, 2000), was adopted:

$$F(x) = \frac{1}{2} erfc\left[-\frac{\ln x - \lambda}{\zeta\sqrt{2}} \right] \tag{3.3}$$

where F(x) is the lognormal CDF, *erfc* is the error function, λ and ζ are the lognormal distribution parameters. Therefore, the fragility function that has to be derived is completely described once λ and ζ are found. Based on Rota (2007), these parameters were found using a nonlinear least-square optimization algorithm and a lognormal CDF function to fit the data obtained with Equation (3.2).

Fragility curves were obtained for both mechanisms: horizontal sliding and overturning failure, i.e. for RHD and residual tilt. Three geometric configurations were also considered, respectively for W/H ratios of 0.64, 0.88 and 1.12. The entire process was followed also using results from an ANN calibrated on analyses were liquefaction occurrence was prevented. This was modelled in FLAC by disabling the dynamic pore pressure increment and the shear strength decrease under seismic excitation. In this way, fragility curves were derived for both stable and liquefiable soils.

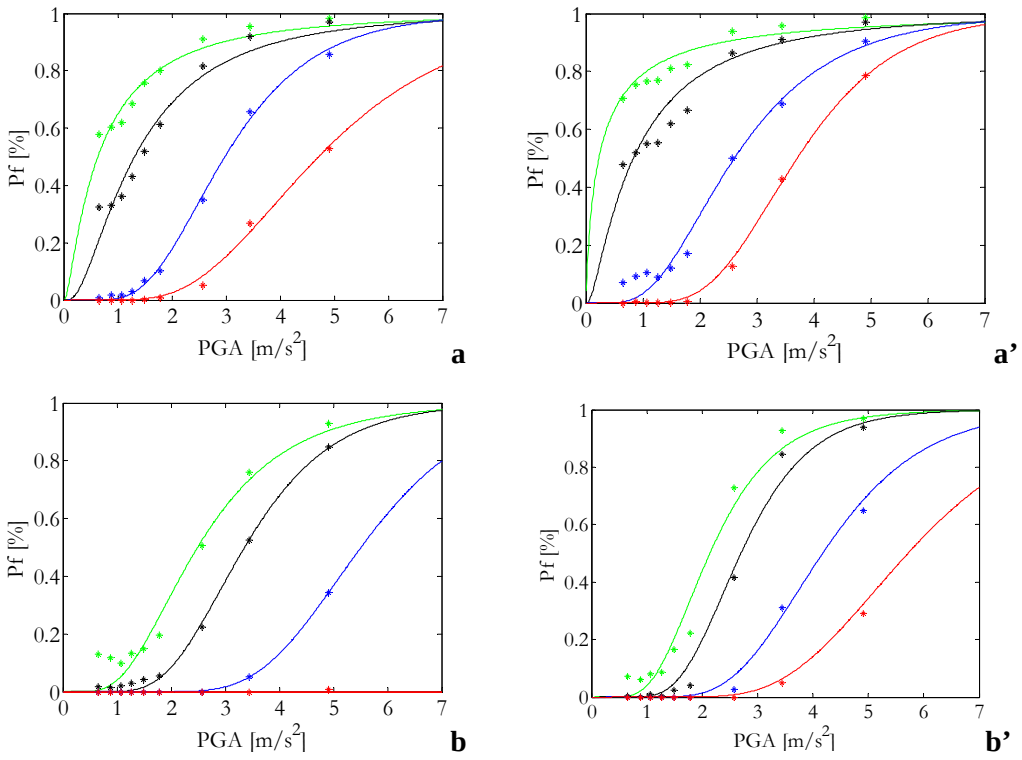

Figure 9. Comparison of RHD fragility curves for two different configurations (base width/height ratios, W/H) without (left side) and with (right side) liquefaction modelling. From the left top to the right down, are represented: a) W/H=0.64, without liquefaction; a') W/H=0.64, with liquefaction; b) W/H=1.12, without liquefaction; b') W/H=1.12, with liquefaction. The considered DS are those of Table 1.2. The marks on the plots represent the observational cumulative failure frequencies obtained with the ANN.

Figure 9 represents the RHD fragility curves for both stable and liquefiable soils conditions, for all DS, and for W/H ratios of 0.64 and 1.12. The interested reader can find the curves for W/H=0.88 and the ones for tilt in Calabrese and Lai (2012), together with several comparisons between the curves of each considered configuration at every DS.

ACKNOWLEDGMENT

The research has been carried out under the financial auspices of the Department of Civil Protection of Italian Government (Progetto Esecutivo 2009–2012, progetto d5 – Vulnerabilità e Rischio Sismico di Opere Portuali Marittime). Such support is gratefully acknowledged by the authors. The first author would also like to express his appreciation to the Italian Air Force for the research leave to join the PhD program of the ROSE School.

REFERENCES

Baker, J.W. (2007). Correlation of ground motion intensity parameters used for predicting structural and geotechnical response. Applications of Statistics and Probability in Civil Engineering, Kanda, Takada, Furuta (eds.), Taylor & Francis Group, London, United Kingdom.

Byrne, P.M. (1991). A cyclic shear volume coupling and pore-pressure model for sand. *Second International Conference on Recent Advances in Geotechnical Earthquake Engineering and Soil Dynamics*, Paper No. 1.24, pp. 47-55.

Calabrese, A. and Lai, C.G. (2012). Performance-Based Seismic Design and Fragility Evaluation of Blockwork Wharf Structures. Research Report Rose 2012. IUSS Press, Pavia, Italy.

Corigliano M., Lai C.G., Rota M., and Strobbia C. (2012). ASCONA: Automated Selection of Compatible Natural Accelerograms. *Earthquake Spectra*, In press.

Demuth, H., and Beale M. (2004). Neural Network Toolbox for Use with MATLAB, The MathWorks, Inc., Natick, Massachusetts, USA.

Hajela, P., Fu, B., and Berkle, L. (1992). Neural networks in structural analysis and design: An overview. *Computing Systems in Engineering* **3:1-4**, 525-538.

Itasca (2000). FLAC (Fast Lagrangian Analysis of Continua). Itasca Consulting Group Inc., Minneapolis, Minnesota, USA.

Jones, A.L., Kramer, S.L., and Arduino, P. (2002). Estimation of uncertainty in geotechnical properties for performance-based earthquake engineering. Report 2002/16. Pacific Earthquake Engineering Research Center, University of California, Berkeley.

Lee, T.-H., and Mosalam, K.M. (2005). Seismic demand sensitivity of reinforced concrete shear-wall building using FOSM method. *Earthquake Engineering and Structural Dynamics* **34:14**, 1719-1736.

Lysmer, J., and Kuhlemeyer, R. L. (1969). Finite dynamic model for infinite media, *Journal of Engineering Mechanics* **95:4**, 859-877.

Martin, G.R., Finn, W.D.L., and Seed, H.B. (1975). Fundamentals of liquefaction under cyclic loading. *Journal of Geotechnical Engineering Division, ASCE* **101**, pp. 423-438.

PIANC (2001). Seismic Design Guidelines for Port Structures. International Navigation Association, A.A. Balkema Publishers, Lisse, the Netherlands.

Rathje, E.M., and Saygili, G. (2008). Probabilistic seismic hazard analysis for the sliding displacement of slopes: scalar and vector approaches. *Journal of Geotechnical and Geoenvironmental Engineering* **134:6**, 804-814.

Rota, M. (2007). Advances in the derivation of fragility curves for masonry buildings. PhD thesis. European School for Advanced Studies in Reduction of Seismic Risk (ROSE School), Pavia, Italy.

Scarpelli, G., and Piersigilli, J. (2005). Lavori di escavo del canale e del bacino del porto di GioiaTauro. Documenti Progettuali. Autorità Portuale di Gioia Tauro, Italy (in Italian).

Seed, H.B., Wong, R.T., Idriss, I.M., and Tokimatsu, K. (1986). Moduli and damping factors for dynamic analyses of cohesionless soils. *Journal of the Geotechnical Engineering Division, ASCE* **112:GT11**, 1016-1032.

Shinozuka, M., Feng, M.Q., Lee, J., and Naganuma, T. (2000). Statistical analysis of fragility curves. *Journal of Engineering Mechanics* **126:12**, 1224-1231.

The MathWorks (2007). MATLAB version 7.5.0. The MathWorks, Inc., Natick, Massachusetts, USA.

Westergaard, H. M. (1933). Water pressure on dams during earthquakes. *Transactions of ASCE* **98**, 418-433.